Drug Delivery and Translational Research (2020) 10:1019–1031
https://doi.org/10.1007/s13346-019-00702-6

ORIGINAL ARTICLE

Exploring micellar-based polymeric systems for effective nose-to-brain drug delivery as potential neurotherapeutics

Varsha Pokharkar[1] · Smita Suryawanshi[1] · Vividha Dhapte-Pawar[1]

Published online: 19 December 2019

Abstract

Non-invasive nose-to-brain delivery presents a competitive strategy for effective drug targeting. This strategy can potentially evade the blood-brain barrier (BBB) depending on the pathway the drug and/or drug/micelle composite travels, thereby allowing direct drug delivery to the brain. This delivery strategy was employed for lurasidone, a clinically USFDA-approved neurotherapeutic molecule in bipolar disorders and schizophrenia treatments. The aim of this study was to develop mixed polymeric micelles of lurasidone HCl (LH) for targeted brain delivery via intranasal route. Lurasidone HCl-loaded mixed micelles (LHMM) were prepared by solvent evaporation method and optimized by 3^2 factorial design to quantify the effects of excipients on micelle size and entrapment efficiency. Fourier transform infrared spectroscopy helped in scrutinizing drug-excipient interactions whereas transmission electron microscopy images showed particle size and shape. Further, LHMM and LHMM hydrogel were evaluated for in vitro diffusion, histopathology, ex vivo permeation, in vivo pharmacokinetics and stability studies. Optimized LHMM exhibited 175 nm particle size and 97.8% entrapment efficiency with improved in vitro drug diffusion (81%). LHMM hydrogel showed 79% ex vivo drug permeation without any significant signs of nasociliary toxicity to sheep nasal mucosa. Single dose in vivo pharmacokinetic studies showed improved therapeutic concentration of drug in the brain post intranasal administration with 9.5 ± 0.21 μg/mL C_{max} and $T_{1/2}$ of 19.1 ± 0.08 h as compared to pure drug. LHMM, when administered by intranasal route, demonstrated significant increase in the drug targeting efficiency as well as potential (%DTE and %DTP) of drug as compared to pure lurasidone. Thus, nanosized mixed micelles were useful in effective brain delivery of lurasidone HCl via intranasal route.

Keywords Lurasidone · Mixed micelles · Intranasal route · Factorial · Pharmacokinetics

Introduction

Psychotic disorders pose a major health challenge and are one of the leading causes of poor psycho-social function worldwide [1]. As per World Health Organization (WHO) reports, more than 26 million individuals suffer from schizophrenia [2]. Schizophrenia, one of the most debilitating chronic psychiatric disorders, causes dementia, delirium or hallucinations in the late adolescence or early adulthood. It is known to affect more than 1% of the global population. Atypical antipsychotics recognized to regulate the dopamine dysfunction within the brain are used to treat schizophrenia. However, they suffer from weight gain, increased risk of diabetes, elevation in the metabolic abnormalities and like extra pyramidal symptoms [3]. Hence, second-generation atypical antipsychotics are preferred to provide more benefit with minimum risk.

Lurasidone hydrochloride (LH) [(3aR,4S,7R,7aS)-2-{(1R,2R)-2-[4-(1,2-benzisothiazol-3-yl) piperazin-1-ylmethyl]cyclohexylmethyl} hexahydro-4,7-methano-2H iso indole-1,3-dione hydrochloride] is a novel benzisothiazol derivative approved by USFDA in bipolar disorders and schizophrenia treatments [4]. It is most effective in cases where muscle tremors, orthostatic hypotension and hyperprolactinaemia are major issues of concern. As compared to the typical and conventional, atypical antipsychotic agents, the newer atypical agents like lurasidone present the prospective benefits of lesser extrapyramidal adverse effects,

✉ Varsha Pokharkar
varsha.pokharkar@bharatividyapeeth.edu;
vbpokharkar@yahoo.co.in

[1] Department of Pharmaceutics, Poona College of Pharmacy, Bharati Vidyapeeth University, Erandwane, Pune, Maharashtra 411038, India

positive metabolism and feasibility of sublingual administration for patients with history of noncompliance towards 'cheeking' medications or a dysphagia. Commercially available lurasidone formulation is an oral tablet marketed as Latuda®, known to act on the D2 and 5-HT2A receptors as antagonist and show its antipsychotic action [5]. LH delivery suffers from the extensive first pass metabolism (40%) and less (9–19%) oral bioavailability in the humans [6] due to low aqueous solubility (BCS class II drug) [7]. Also, this oral dosage form needs to be taken with the food (minimum 350 cal) for absorption from gastrointestinal tract. Schizophrenic patients often consume less food leading to noncompliance with this medication [1]. As brain is the site of action for LH, blood-brain barrier (BBB) limits the drugs from reaching at the site, leading to therapeutic failure. Therefore, alternate strategies are required to overcome these limitations of conventional LH formulations for effective treatment of the neurodegenerative disorders.

Many researchers have experimented with solubility and dissolution enhancement techniques to increase LH bioavailability using formulation strategies like solid dispersions [7], co-amorphous system [6], nanocrystals [3], self-micro emulsifying drug delivery system (SMEDDS) [8], self-nanoemulsifying drug delivery systems (SNEDDS) [9], nanosuspensions [10] and lipid carriers of LH [11]. These novel drug delivery systems may possess few challenges related to manufacturing intricacies and economic feasibility in commercial production. However, there is a need of increasing the targeting efficiency and potential of LH wherein solubility, bioavailability and first pass metabolism issues will also be addressed.

Among the various strategies utilized in brain targeting, nasal route has more advantages as a non-invasive technique of surpassing BBB [12]. It offers rapid absorption via olfactory region of the nasal cavity leading to fast action. Polymeric micelles show better targeting and transportation to brain via intranasal route which aids in better clinical translation of essential therapeutic molecules like LH [13]. Micelles having hydrophobic core with a hydrophilic shell are more stable than the typical surfactant-based drug delivery systems. Due to more micellar stability and better drug loading efficiency, mixed micelles are preferred over single polymer micelles [14]. Mixed micelles ensure aqueous solubility of nanosystems and thermodynamic stability as well as enhanced drug solubilizing potential than other novel drug delivery systems like lipid carriers, solid dispersions, nanocrystals, SMEDDS and SNEDDS. Mixed polymeric micelles are known to overcome the physiological barriers (like nasal, ocular) by enhancing the permeation and improving the residence time on the barrier surface [15].

Our design rationale for improving brain targeting of LH was to formulate it as mixed polymeric micelles administered via intranasal route. Such formulation strategy is expected to elevate LH bioavailability in brain and achieve effective therapeutic levels. This study aimed at developing LH-loaded mixed micelles (LHMM) with desirable properties. 3^2 factorial designs helped in optimizing the experimental design as well as assessing the effects of different formulation variables on the expected properties of LHMM with minimum number of experiments. Optimized, stable LHMM were evaluated for bioavailability enhancement using drug diffusion studies, in vivo efficacy in rats along with ex vivo permeation and histopathological studies in nasal mucosa.

Materials and methods

Materials

LH was purchased from Watson Pharmaceuticals Ltd., India. Gelucire 44/14 (GL44) was generously supplied by Gattefosse, India, and Pluronic F127 (PF127) was gifted by BASF, India. Carbapol-940 was procured from HiMedia Laboratories Pvt. Ltd., Mumbai, India. Solvents like acetonitrile and methanol procured from Merck, India, were of HPLC grade. All other chemicals of analytical grade were used. Milli-Q water (Millipore, MA) was used during HPLC analysis.

Animals

Wistar male rats (weighing 200–250 g) were purchased from National Institute of Biosciences, Pune, India, and used for in vivo pharmacokinetic studies [5]. Pharmacokinetic study protocol was prepared as per the guidelines of Committee for the Purpose of Control and Supervision of Experiments on Animals and approved by the Institutional Animal Ethics Committee (IAEC) of Bharati Vidyapeeth University, Pune (CPCSEA/PCP/PCT15/2017-2018). Animals were maintained under conventional housing conditions in plastic cages with free access to standard rat diet and water at temperature of 24 ± 1 °C under 12-h light/dark cycle and RH of 55 ± 5%. They were fasted overnight prior to experimentation.

Methods

Critical micelle concentration determination

Dye micellization method was used to determine the critical micelle concentration (CMC) of polymers using Sudan IV dye [16, 17]. Polymer solutions (1–10 μg/ml) were prepared, mixed with Sudan IV dye followed by addition into chloroform in 5:1 proportion. Aqueous layer collected post centrifugation (1000 rpm for 1 h) was further analysed by the UV spectrophotometer at 350 nm. CMC value was determined from the graphical plot of absorption intensity against the polymeric concentration.

Preparation of LH mixed micelles

LH mixed micelles (LHMM) were prepared by the solvent evaporation method [18]. The findings of CMC-based preliminary studies and drug-excipient compatibility analysis helped in selection of the excipients. Pluronic F127 (PF127) and Gelucire 44/14 (GL44) were selected as micelle forming agents. Drug and excipients (PF127, GL44) were dissolved in 3 ml methanol and added dropwise in 10 ml distilled water with simultaneous sonication at 130 W for 3 min using probe sonicator. The resultant dispersion was filtered through 0.45-μm filter to remove impurities; sediments on the filter were further dissolved in ethanol in order to determine the percent of precipitated LH.

Optimization of LHMM by factorial design

Factorial designs help in assessing the effects and cross effects of individual variables using minimum experiments to reduce errors. Effect of drug amount (X_1) and excipients PF127:GL44 ratio (X_2) was found to significantly affect both dependent variables, micelle size (Y_1) as well as entrapment efficiency (EE) (Y_2). Hence, they were selected as independent factors. 3^2 factorial design was applied to assess the effect of independent factors on the dependent factors and correlate the underlying mechanisms [19]. 3^2 factorial design was applied during optimization of LHMM to derive the relationships between variables through minimum experimentation as depicted in Table 1.

The design composed of nine experimental runs was analysed using Design Expert software (version 11) to obtain an empirical Eq. (1) as follows:

$$Y = b_0 + b_1X_1 + b_2X_2 + b_{11}X_1^2 + b_{22}X_2^2 + b_{12}X_1X_2 \quad (1)$$

where Y is the dependent variable, b_0 is the arithmetic mean response of all quantitative outcomes of 9 runs and b_1 and b_2 are the corresponding coefficients of factors X_1 and X_2, respectively; interaction term X_1X_2 showed the changes in response when both factors are changed simultaneously. Polynomial terms (X_1^2 and X_2^2) indicate nonlinearity in responses.

Preparation of LHMM hydrogel

Nasal mucociliary clearance needs to be considered while designing formulations for intranasal delivery [20]. Hydrogels are established as elastic polymer matrix, useful in physical entrapment of active molecules. Active moieties are encapsulated into hydrogel to address the mucosal clearance issue, for ease of application and increase in the residence time. Measured amount of drug was added in carbopol-945/glycerine gel to obtain an optimum viscosity. Weighed quantity of carbopol-940 (5%) was dispersed in distilled water under mild stirring and allowed to swell for 24 h followed by addition of glycerine and neutralization. Resultant transparent gel was stored for 24 h at room temperature to stabilize. LHMM hydrogel was prepared by simple mixing of LHMM dispersion and hydrogel matrix under mechanical mixing (25 rpm) for 10 min [21]. Viscosity measurements of LHMM gel were monitored using thermostatically controlled Brookfield viscometer (DV3T Rheometer, USA) with various spindles.

Characterization of LHMM

Fourier transform infrared spectroscopy

Fourier transform infrared spectroscopy (FTIR) spectrophotometer (JASCO FTIR- V4100, Japan) was used for obtaining

Table 1 Effects of formulation variables on micelle size and % EE of lurasidone hydrochloride-loaded mixed micelles (LHMM) by 3^2 factorial design

Formulation batches	Coded levels (actual values)		Particle size (nm)	% EE*
	X_1 (drug content in mg)	X_2 (PF127: GL44)*	Y_1	Y_2
F1	− 1(2)	− 1(0.5)	225 ± 0.02	98.35% ± 0.01
F2	0(5)	− 1(0.5)	442 ± 0.014	98.08% ± 0.004
F3	1(8)	− 1(0.5)	708 ± 0.06	93.13% ± 0.08
F4	− 1(2)	0(1)	250 ± 0.21	97.81% ± 0.034
F5	*0(5)*	*0(1)*	*175 ± 0.07*	*97.8% ± 0.009*
F6	1(8)	0(1)	686 ± 0.062	94.18% ± 0.02
F7	− 1(2)	1(2)	274 ± 0.031	97.51% ± 0.07
F8	0(5)	1(2)	468 ± 0.032	97.68% ± 0.05
F9	1(8)	1(2)	992 ± 0.01	96.51% ±0.07

Values given as mean ± standard deviation, $n = 3$

**EE* entrapment efficiency, *PF127* Pluronic F127, *GL44* Gelucire 44/14

#Batch F5 with highest %EE and lower particle size was selected as an optimized batch

infrared spectra of LH, PF127, GL44 and LHMM samples by KBr pellet method up to 4000 cm^{-1}.

Micellar morphological study

Mean micelle size of LHMM was analysed using particle size analyser based on laser diffraction technique (Malvern Mastersizer 2000SM version 5.22, Malvern Instruments Corp., UK). Morphology of LHMM was screened using transmission electron microscope (TEM) (Hitachi H 7500, Houston, TX) working on accelerating voltage of 100 kV. A droplet of sample was added to a copper grid; excess liquid was removed followed by drying under IR lamp and viewed under microscope.

Entrapment efficiency

Micellar dispersion was subjected to centrifugation (13,000 rpm for 40 min), after which the micelles were separated [22]. By using UV spectrophotometer, free drug was estimated from supernatant at 230 nm. % EE was calculated using the formula mentioned in Eq. 2

$$\%EE = \frac{W_{\text{Initial drug}} - W_{\text{Free drug}}}{W_{\text{Initial drug}}} \times 100 \quad (2)$$

where $W_{\text{Initial drug}}$ is the amount of drug added and $W_{\text{Free drug}}$ is the amount of free drug in supernatant after centrifugation.

In vitro diffusion study

Drug diffusion study from LHMM was performed by dialysis bag method in USP type II dissolution apparatus (Lab India DS 8000, Mumbai, India). LHMM and aqueous LH dispersion containing equivalent amount of drug (2.5 mg) were placed into a dialysis bag (MW cutoff 12–14 kDa). This dialysis bag was subjected to 500 ml phosphate buffer (pH 6.4) media at 37 ± 0.5 °C under continuous stirring at 100 rpm. At predetermined time intervals (0.5, 1, 2, 4, 6, 8 and 12 h), 2-ml aliquots were withdrawn while the sink conditions were maintained with an equal volume of fresh dissolution medium containing 5% Tween 80. The samples were diluted and analysed in triplicate to determine the diffused drug using UV-visible spectrophotometer at 230 nm. Percent (%) cumulative drug release was plotted against time to understand the release profile and its underlying mechanism.

Ex vivo permeation study

Franz diffusion cells were used for performing ex vivo permeation study on the sheep nasal mucosa obtained from local slaughter house as a permeation barrier. It was cleaned and allowed to equilibrate in phosphate buffer (pH 6.4) for 20 min. Acceptor compartment was filled with phosphate buffer and nasal mucosa with 0.2-mm thickness mounted over diffusion cell. Pure LH dispersion and LHMM hydrogel containing equal amount of drug were placed on to nasal mucosa mounted on donor compartment. During the permeation study, 37 ± 0.5 °C temperature was maintained using recirculating water bath and aerated with carbogen gas at a rate of 1–3 bubbles per second which supplies oxygen for improving viability of tissue throughout the experiment. Aliquots from the receptor phase were sampled at periodic interval of 1, 2, 3, 4, 6, 8 and 10 h and replaced with fresh phosphate buffer. Subsequent dilutions were made and mean values of LH permeated were assessed to understand the permeation behaviour of LHMM. The amount of LH permeated into the receptor compartment from the pure LH dispersion and LHMM hydrogel was determined by UV-visible spectrophotometer at 230 nm. Flux, the amount of LH released per area of permeation through sheep nasal mucosa was measured from the ex vivo permeation study.

Histopathological study

Nasal mucosa of sheep except the septum part was sectioned into two pieces (P_1 and P_2) with 0.2-mm thickness [23, 24]. P_1 was treated with negative control (phosphate buffer pH 6.4) whereas P_2 received LHMM hydrogel. After this 10-h treatment, samples were washed with buffer and preserved in 10% neutral formalin for 24 h. Later, these samples were cut into 4 mm wide sections, vertically and embedded in paraffin wax. These sections were stained with haematoxylin-eosin to evaluate any damage to nasal mucosa using microscopic observations.

In vivo pharmacokinetic and brain distribution study

Animals were randomly divided into four groups ($n = 18$ in each group). Prior to drug administration, animals were anaesthetized with thiopental (intraperitoneal injection). A dose equivalent to 1 mg/kg of LH and LHMMs was administered intravenously (IV) across the tail vein to the respective group [5]. Intranasal (IN) dose in rats was administered using a cannula placed 10–15 mm inside nasal cavity and connected to a 100-μL micropipette. Blood samples (1 ml) and brain tissues were separated at 0.5, 1, 1.5, 2, 3, 4, 6, 10 and 24 h after IV and IN administration and subjected to di-sodium EDTA to prevent clot formation. Brain tissues were homogenized using 5 mL ice-cold physiological saline. After centrifugation at 15000 rpm, 4 °C temperature for 15 min, separated plasma and brain homogenates were stored at − 70 °C until further analysis. LH concentrations in plasma and brain tissue were analysed after liquid-liquid extraction using HPLC system (LC-20, AT, Shimadzu, Kyoto, Japan). The chromatographic system operation and recording of data were performed using Borwin software. Mobile phase composing

phosphate buffer (pH 3, 20 mM):acetonitrile:methanol (55:10:35, v/v/v) was filtered through 0.45-μm filter using vacuum and degassed for 15 min by bath sonication. It was delivered into HPLC system at 1.2 mL/min flow rate. Chlorpromazine was used as an internal standard (IS). Compounds were monitored by UV-visible detector (Jasco UV 2075) at 230 nm.

To evaluate brain targeting of LHMM after IV and IN administration, the following parameters were calculated:

DTE % - Drug targeting efficiency: time average partitioning ratio of drug

DTP % - Drug targeting potential: direct nose-to-brain transport of drug were calculated by using following formulae (Eq. 3 and Eq. 4)

$$\mathrm{DTE}\% = \left[\frac{\left(\frac{\text{AUC brain}}{\text{AUC blood}_{\mathrm{IN}}}\right)}{\left(\frac{\text{AUC brain}}{\text{AUC blood}_{\mathrm{IV}}}\right)}\right] \times 100 \quad (3)$$

$$\mathrm{DTP}\% = \left(\frac{B_{IN} - B_x}{B_{IN}}\right) \times 100 \quad (4)$$

where Bx represented the fraction of brain ($AUC_{0\text{-}t}$) contributed by systemic circulation post intranasal administration:

$$B_x = \left(\frac{B_{IV}}{P_{IV}}\right) \times P_{IN} \quad (5)$$

B_{IV} is the brain $AUC_{0\text{-}t}$ after intravenous administration of LH or LHMM.

B_{IN} is the brain $AUC_{0\text{-}t}$ after intranasal administration of LH or LHMM.

P_{IN} is the blood $AUC_{0\text{-}t}$ after intranasal administration of LH or LHMM.

P_{IV} is the blood $AUC_{0\text{-}t}$ after intravenous administration of LH or LHMM.

Statistical data analysis

Non-compartmental analysis was performed for various pharmacokinetic parameters considering each individual set of data using WinNonlin version 4.0 (Pharmsight, Mountain View, CA, USA) pharmacokinetic software.

Stability study

Freeze dried LHMM was stored in 5-ml glass vials, tightly sealed with plastic closures. These glass vials were placed in stability chamber at 25 °C and accelerated conditions (40 °C and 75% RH) for 3 months. LHMM samples were withdrawn and analysed for change in micellar size and %EE at regular intervals.

Results and discussion

CMC determination

The CMC of PF127 and GL44 was found to be 0.008% w/v and 0.0006% w/v, respectively (Fig. 1). Combining GL44 and PF127 resulted in significant decrease in CMC, i.e. 0.0005% w/v ($p < 0.05$). Sudan IV dye was used to detect the sudden increase in absorbance which marked the formation of

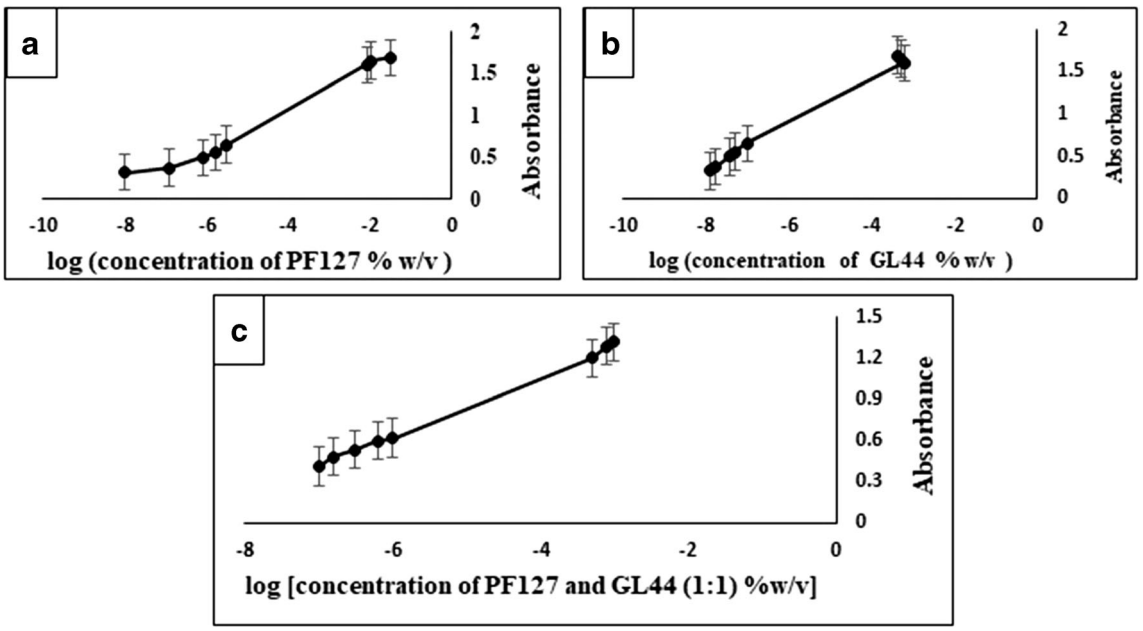

Fig. 1 Critical micelle concentration (CMC) plots of **a** Pluronic F127 (PF127), **b** Gelucire 44/14 (GL44) and **c** PF127-GL44 combinations

micelles above CMC, due to its location in the micellar core. CMC of excipients is inversely related to hydrophobic interactions. GL44 aids in lowering the CMC of mixed micelles owing to its more hydrophobic interactions between laurate chains and polymeric chains of PF127 [19]. These hydrophobic interactions balanced with hydrophilic portion of all the excipients imparted better stability to micelles [24].

Optimization of LHMM

Micelles formation may not occur if the hydrophobic content in the system is too high while rise in hydrophilic region leads to destabilization of the system [25]. Hence, selection of optimum amount of the polymers plays a key role for micellar stability. In micellar system, agglomeration of particles occurs due to excess drug content which start leaching. Hence, stability of the formulation is important to incorporate maximum amount of drug. 3^2 factorial design was applied to study the optimum amount of excipients and drug required for stable LH-loaded micellar formulation as evaluated from the micelle size and % EE as dependent variables (Table 1).

Micellar size

The micellar size is known to show predominant impact on drug release. Contour plot shown in Fig. 2(a) illustrated the statistically significant relationship between dependent and independent variables.

The regression equation for this response is represented using empirical model Eq. 6 which reveals the quantitative effects of formulation components, X_1 and X_2 on micellar size (Y_1). Regression coefficient (R^2) values of 0.9923 ascertain the significance of this model.

$$Y_1 = 267.07 + 280.11*X_1 + 159.83*X_2 + 60.83*X_1^2 + 43.88*X_2^2 + 65.46*X_1X_2 \quad (6)$$

The b_0 coefficient indicated an average micellar size of 267.07 nm. When the coefficients of the two independent variables and the interaction terms were compared (Eq. 6), values for individual terms ($X_1 = +280.11$, $X_2 = +159.83$) were greater than interaction terms ($X_1^2 = 60.83$, $X_2^2 = 43.88$, $X_1X_2 = 65.46$). This implied that independent variables (X_1 and X_2) are major contributing factors than their combination (X_1X_2, X_1^2, and X_2^2) in defining the size of LHMMs. Also, the positive coefficients indicate direct impact of the drug content and PF 127:GL44 ratio on the micellar size wherein increased amount of drug as well as excipients increased the micelle size.

Contour plots showed the predicted particle size values at different levels of excipients' ratio and drug concentrations (Fig. 2(a)). At higher drug concentrations, the increase in hydrophobic drug core diameter may have resulted in increased micellar diameter. This effect was attributed to the increased drug content that caused the core to stretch. Beyond certain extent, the drug precipitated out resulting into a particle size beyond 1 μm due to their agglomeration. Both the excipients showed direct relation with particle size which could be ascribed to the swelling of outer micelle shell [26]. Further, the extrapolation effect of both the parameters ($X_1^2 = 60.83$ and $X_2^2 = 43.88$) showed an increase in the particle size. Sufficient quantity of surfactant helped in increasing the stability of micelles by preventing the agglomeration of particles [27]. Based on this, batch *F5* was optimized for further characterization.

The morphology of LHMM captured by TEM revealed uniform, spherical morphology with the micellar structure as depicted in Fig. 3(a). This typical spherical shape of nanosized mixed micelles with darker outside layer is attributed to the difference between the drug and micellar layers (related to the excipients) density [28]. The observed mean diameter was less than 200 nm, which is well correlated with the particle size obtained with particle size analyser. A clear identification of the micelle particles without any agglomeration is shown in Fig. 3(b).

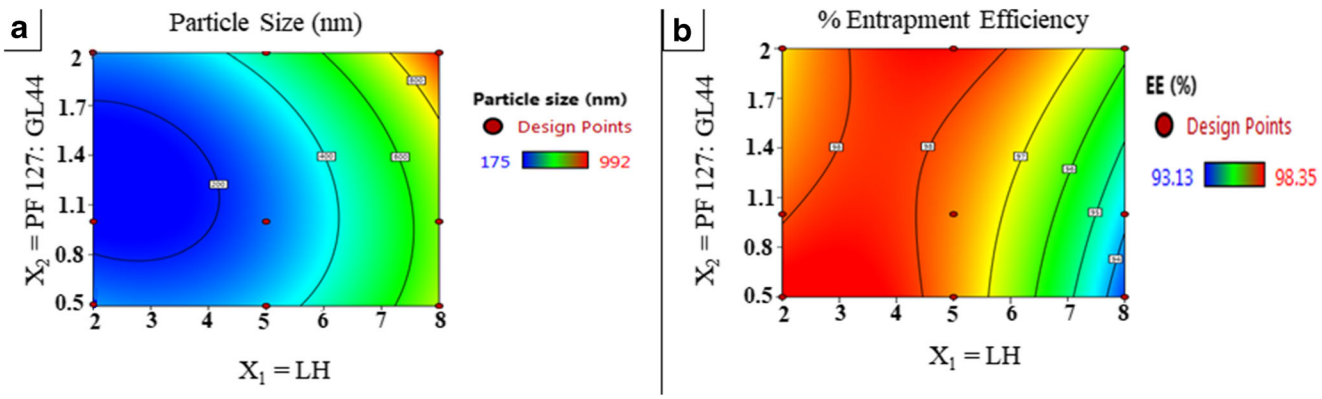

Fig. 2 Contour plots to study the effects of independent variables, drug lurasidone hydrochloride (LH) content (X_1) and Pluronic F127 (PF127): Gelucire 44/14 (GL44) ratio (X_2) on **a** micellar size and **b** % entrapment efficiency (EE)

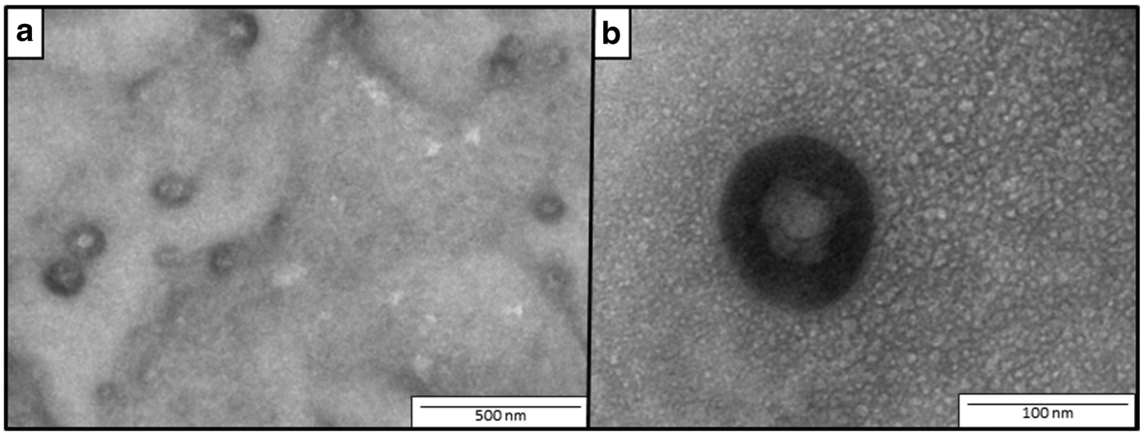

Fig. 3 TEM images of lurasidone hydrochloride-loaded mixed micelles (LHMM) **a** micellar distribution and **b** Single micelle structures

Entrapment efficiency (%EE)

The %EE of LHMM was found in the range of 93.13 ± 0.08 to 98.35 ± 0.01%. The influence of independent factors on %EE proved to be statistically significant ($p < 0.01$) and presented in Eq. 7 and Fig. 2(b).

$$Y_2 = 97.77–1.53*X_1 + 0.3567*X_2–1.61X_1^2 + 0.1812*X_2^2 + 1.05*X_1X_2 \quad (7)$$

High regression coefficient R^2 (0.996) showed excellent correlation between the amount of drug and polymers on EE, establishing the significance of model.

The regression Eq. 7 of response Y_2 showed negative relationship with drug ($X_1 = 1.53$) and positive relationship with PF 127:GL44 ratio ($X_2 = 0.3567$). When the amount of drug (X_1) was increased, the EE lowered even when this effect was extrapolated (X_1^2).

Contour plots showed the predicted %EE values at different levels of excipients ratio and drug concentrations (Fig. 2(b)). This behaviour was attributed to the decreased capacity of polymer molecules to hold the excess amount of drug molecules beyond 5 mg. When X_2 increased, EE decreased for lower level of X_1. Hydrophobicity associated with GL44 is known to enhance the drug partitioning in hydrophobic core of micelles [19]. Increased EE is attributed to the balance among the adhesive forces in hydrophobic part of micelle and cohesive forces in outer hydrophilic part. Cohesive and adhesive forces of core (lauric acid chains, tryglycerides) and repulsive forces existing between the larger polyethylene glycol (PEG) chains of GL44 in the outer shell of micelles are known to occur at high concentration of GL44 which in turn

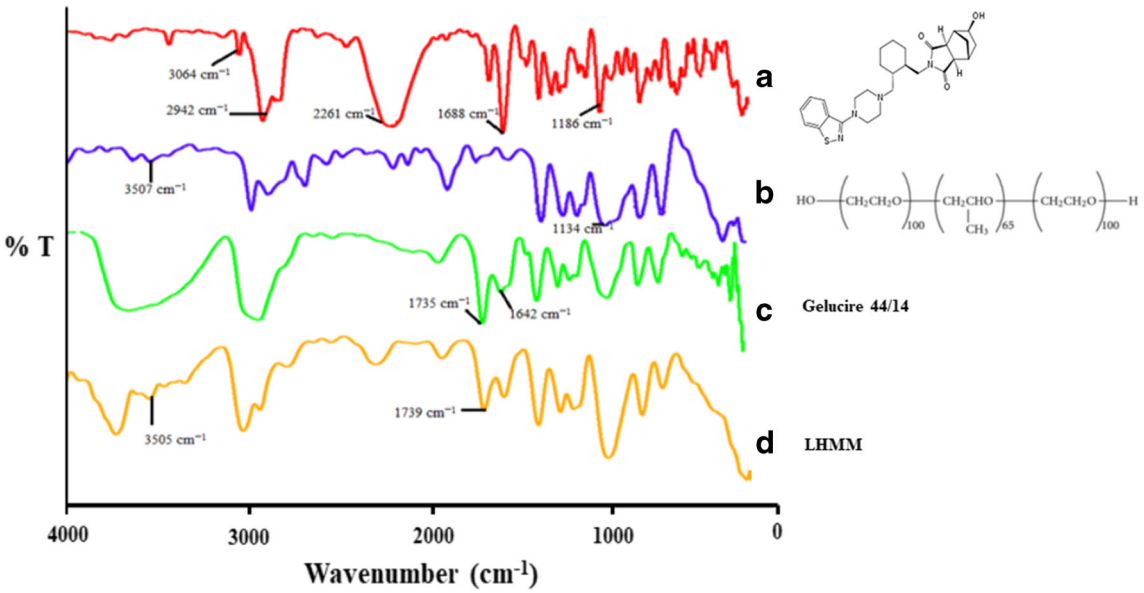

Fig. 4 FTIR spectra of **a** drug lurasidone hydrochloride (LH), **b** Pluronic F127 (PF127), **c** Gelucire 44/14 (GL44) and **d** lurasidone hydrochloride-loaded mixed micelles (LHMM)

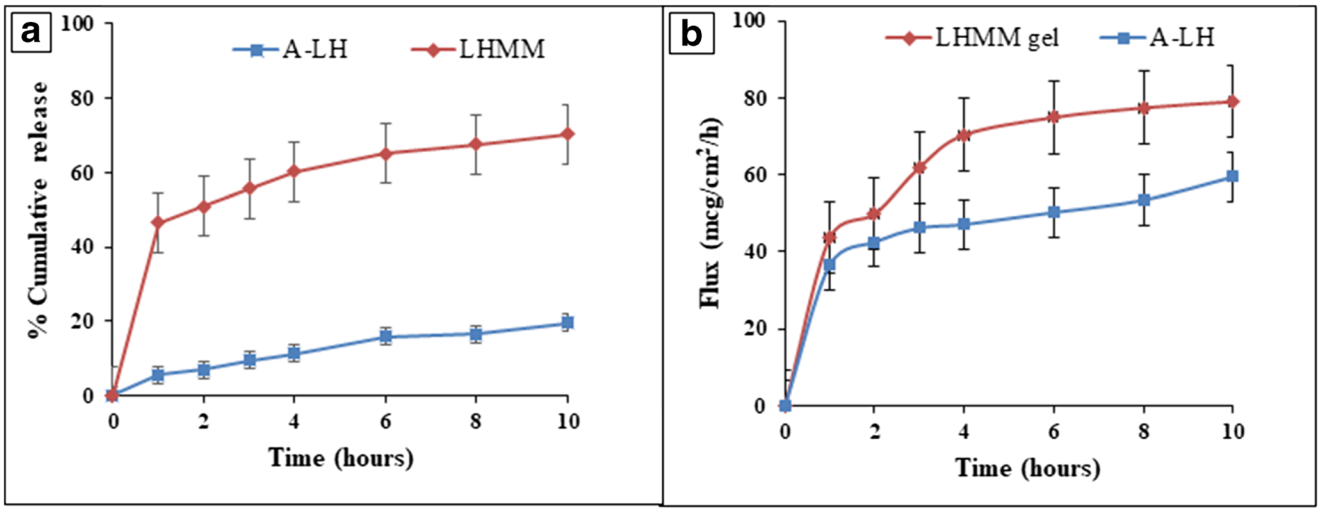

Fig. 5 **a** In vitro drug diffusion study of aqueous lurasidone hydrochloride (A-LH) dispersion and lurasidone hydrochloride-loaded mixed micelles (LHMM). **b** Ex vivo permeation study of lurasidone hydrochloride (A-LH) dispersion and lurasidone hydrochloride-loaded mixed micelles (LHMM) gel

causes increase in EE. Combined effect of X_1 and X_2 (+ 1.05) increased EE of the system, showing a positive correlation. The entrapment of LH in the core is attributed to the solubilizing effect of polymeric core [24]. It was important to incorporate maximum amount of drug along with better stability of the formulation. Highest EE emphasized the selection of Batch *F5* as an optimized batch as it provided a comparably lower particle size. Lower particle sized, polymeric micelles are known to overcome the mechanical clearance with improved physical stability owing to the polymeric coating layer.

Viscosity of LHMM hydrogel was found to be 8000 cP which is in the optimum range at high and low levels of shear rates. This implied that the LHMM hydrogel will possess high viscosity at low shear rate during shelf life whereas it will exhibit free-flowing property during agitation, pouring and spreading owing to low viscosity at high shear rate [1]. With increasing shear stress, micellar-based semisolid system tends to align, in turn elevating the flow for ease of application to nasal mucosa. Hydrogel aids in easy application of LHMM formulation to nasal mucosa while the micellar nanosize with increased surface area is significant in defining the release kinetics. Viscosity of hydrogels aids in understanding the application behaviour; they must have contact with the mucosa for delivery of mixed micelles as against mixed micellar dispersions which may easily drain out from the nasal region.

FTIR study

FTIR spectra of drug, excipients and LHMM illustrated in Fig. 4 confirmed the possibility of interactions among drug and excipients during preparation of mixed micelles. The FTIR spectra of LH showed peak at 3064 cm^{-1} for aromatic C-H vibration, 2942 cm^{-1} for aliphatic group, 2261 cm^{-1} for aryl nitrile peak, 1186 cm^{-1} for C-N stretch and 1688.37 cm^{-1} for C=O stretch. The FTIR spectra of PF127 showed characteristic peaks for hydroxyl (3507 cm^{-1}) and ether groups (1134 cm^{-1}). The characteristic GL44 IR peaks depicted ester (1735 cm^{-1}) and ketone group (1642 cm^{-1}). In LHMM spectra, evident C-H stretch (3064 cm^{-1}) and C-N stretch (1186 cm^{-1}) of drug disappears along with minor shift in the

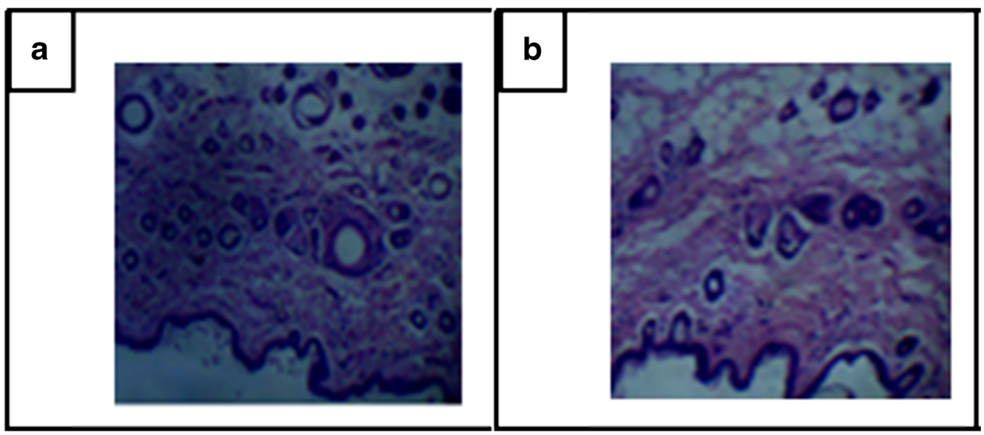

Fig. 6 Histopathological photomicrographs of eosin-haematoxylin stained **a** untreated nasal mucosa and **b** mucosa treated with lurasidone hydrochloride-loaded mixed micelles (LHMM) gel hydrogel

Table 2 Pharmacokinetic parameters after single dose intranasal (IN) and intravenous (IV) administration of pure drug, lurasidone hydrochloride (LH) and lurasidone hydrochloride loaded mixed micelles (LHMM)

Route	Parameters		LH	LHMM
Intranasal	Brain	C_{max} (μg/mL)	0.46 ± 0.04	9.5 ± 0.21***
		T_{max} (h)	1	1
		$T_{1/2}$ (h)	16.2 ± 0.23	19.1 ± 0.08**
		MRT (h)	8.1 ± 0.07	10 ± 0.45
		K_{el} (h^{-1})	0.019 ± 0.32	0.005 ± 0.28
		$AUC_{0-\infty}$ (h × μg/mL)	24.36 ± 1.07	83 ± 1.57***
	Plasma	C_{max} (μg/mL)	1.1 ± 0.76	6 ± 0.57***
		T_{max} (h)	0.03	0.03
		$T_{1/2}$ (h)	11.06 ± 0.1	15.5 ± 0.09*
		MRT (h)	1.59 ± 0.02	1.92 ± 0.36
		K_{el} (h^{-1})	0.06 ± 0.86	0.04 ± 0.03
		$AUC_{0-\infty}$ (h × μg/mL)	35.09 ± 0.62	23.94 ± 0.71**
Intravenous	Brain	C_{max} (μg/mL)	0.64 ± 0.24	3.4 ± 0.31***
		T_{max} (h)	1	1
		$T_{1/2}$ (h)	19.6 ± 0.39	21 ± 0.27**
		MRT (h)	7.8 ± 0.68	9.79 ± 0.53
		K_{el} (h^{-1})	0.035 ± 0.46	0.012 ± 0.08
		$AUC_{0-\infty}$ (h × μg/mL)	17.89 ± 1.04	27.85 ± 0.09**
	Plasma	C_{max} (μg/mL)	2 ± 0.34	9 ± 0.61***
		T_{max} (h)	0.03	0.03
		$T_{1/2}$ (h)	19.8 ± 0.60	11.9 ± 0.39**
		MRT (h)	4.55 ± 0.38	2.07 ± 0.65
		K_{el} (h^{-1})	0.034 ± 0.01	0.06 ± 0.03
		$AUC_{0-\infty}$ (h × μg/mL)	27.6 ± 0.92	31.5 ± 0.87*

All values are presented as the mean ± standard deviation ($n = 6$)

C_{max} maximum concentration; T_{max} time to attain maximum concentration; $T_{1/2}$ half life; *MRT* mean residence time; K_{el} elimination constant; *AUC* area under curve

*$p < 0.05$, **$p < 0.01$, ***$p < 0.001$ considered significant as compared to control group

amine group of drug (from 1186 to 1115 cm^{-1}) and presence of characteristic peaks of PF127 (–OH 3505 cm^{-1}) and GL44 (ester 1739 cm^{-1}, ketone 1642 cm^{-1}) which corroborated the effective encapsulation of the drug in polymeric matrix [29]. This substantiates that there is no major interaction between the drug and other excipients. Minor shift and changes in the intensity of drug peak may be attributed to the molecular dispersion of drug in the surfactant matrix.

In vitro diffusion study

Generally, the drug carriers are known to retard the release rate compared to the drug alone. However, the experimental findings post in vitro diffusion of LHMM were different. Comparative in vitro drug diffusion study illustrated in Fig. 5(a) showed 61% burst drug release within the initial 2 h in PBS (pH 6.4) followed by cumulative 81% release within the next 12 h from LHMM as compared to pure drug dispersion. Drugs like LH with solubility and wettability issues tend to accumulate in the dialysis bag due to the delayed diffusion across the dialysis membrane with subsequent reprecipitation into larger aggregates. So, the overall LH release from pure drug dispersion was merely 30% across the dialysis bag. In the initial 2 h, the LHMM burst release from the mixed micelles occurred. This could be attributed to the fast disruption of the micellar system as a result of higher concentration gradient and cohesion across the dialysis membrane. After the initial release of the LH from the shell or at the core–shell interface, slow release phase occurred corresponding to the LH diffusion from the micellar hydrophobic core. Hydrophilic part of LHMM helps in early permeation of water inside the micelle [19]. Following this preferential uptake, the micelles swell allowing the drug to dissolve and slowly diffuse from hydrophobic part [16]. Polymeric mixed micelles are known to follow Higuchi model ($R^2 = 0.9976$) which defines the drug release across the polymeric matrix by diffusion mechanism.

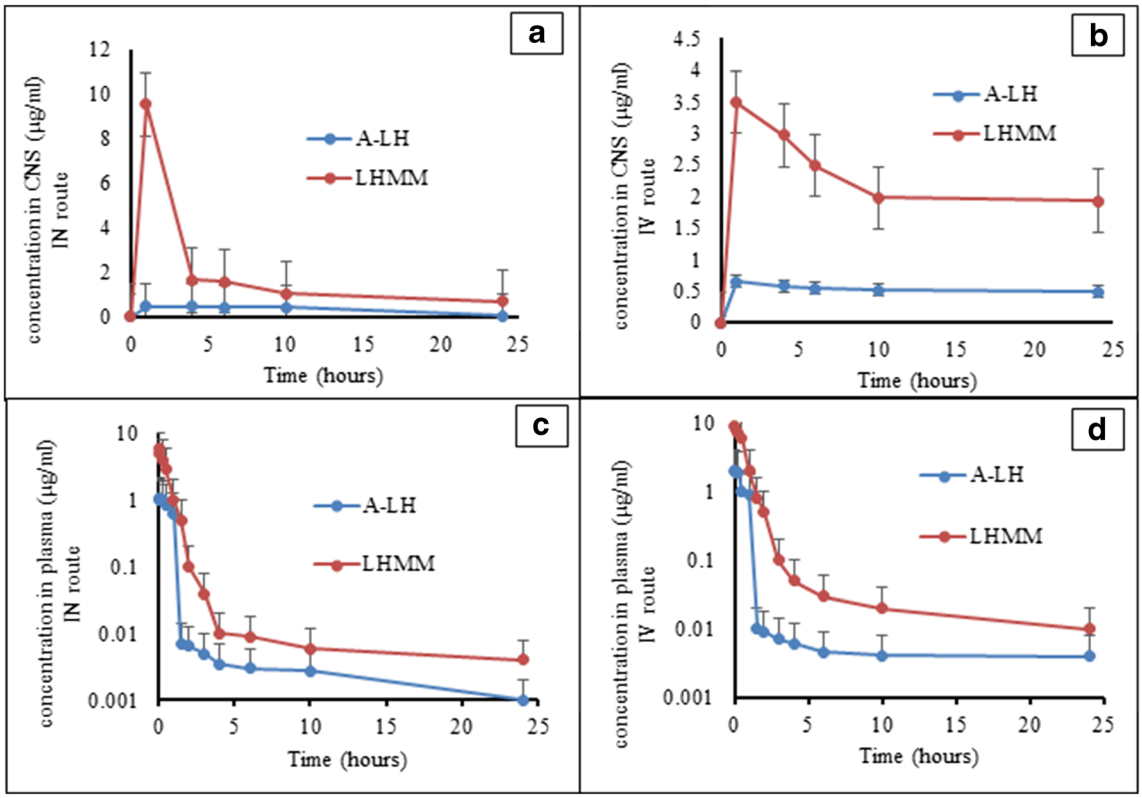

Fig. 7 Plasma and brain concentrations of lurasidone hydrochloride (LH) post intranasal (IN) and intravenous (IV) administration of aqueous lurasidone hydrochloride (A-LH) dispersion and lurasidone hydrochloride-loaded mixed micelles (LHMM)

Significant enhancement in the drug release rate from LHMM was ascribed to the decreased micelle size, which in turn increased the surface area as well as wettability [29, 30]. According to Noyes-Whitney and Prandtl equation, smaller is the particle size, larger is the surface area and shorter is the diffusional distance, which increases the dissolution velocity [31].

Ex vivo permeation study

Permeation study performed in sheep nasal mucosa showed 79 ± 0.02% drug permeation from LHMM gel as compared to 59 ± 0.12% from plain drug suspension after 10 h (Fig. 5(b)). Thus, amount of drug permeated across the biological membrane was increased 1.3 times when it is administered in the form of mixed micelles. Hydrogels are stable, elastic polymeric networks which exhibit distinct swelling ability of LHMM. Enhanced permeation of nanosized, polymeric mixed micelles across the nasal mucosa is attributed to the amphiphilic micellar nanocarrier of LHMM [32]. Non-ionic surfactants present in LHMM reduced the interfacial tension as well as hydrated, fluidized and loosen the intercellular lipid layer of the nasal mucosa to enhance the micellar permeation [33]. Decreased particle size with increased surface area, improved wettability and reduced diffusion layer thickness enhanced the LHMM permeation. Poor wettability, less adhesion and limited contact of free LH affected its permeation across the nasal mucosa.

Table 3 Drug targeting efficiency (DTE) and drug targeting potential (DTP) following intranasal administration of pure drug, lurasidone hydrochloride (LH) and lurasidone hydrochloride-loaded mixed micelles (LHMM)

Batch	DTE (%)	DTP (%)
Pure drug (LH)	107 ± 0.68	6 ± 0.86
Optimized formulation (LHMM)	394 ± 1.03*	74 ± 0.45*

All values are presented as the mean ± standard deviation ($n = 6$)

*$p < 0.01$ considered significant

Histopathological study

The sheep nasal mucosa is similar to the human nasal mucosa, histopathologically [34]. Less significant artefacts related to staining were observed in the microscopic images. Histopathological examination of the sheep nasal mucosa post LHMM treatment did not reveal any signs of nasal toxicity (Fig. 6). It appeared similar to the normal mucosa with intact architecture (no signs of erythema, irritation and edema) in microscopic images. Thus, it was ensured that the developed LHMM formulation was safe for nasal application.

Table 4 Influence of storage condition and duration on particle size (nm) and entrapment efficiency (%EE) of optimized lurasidone hydrochloride-loaded mixed micelles (LHMM)

Months	25 °C (room temperature)		40 °C and 75% relative humidity (RH) (accelerated conditions)	
	Size (nm)	EE (%)	Size (nm)	EE (%)
0	175 ± 0.012	97.8 ± 0.23	175 ± 0.054	97.8 ± 0.038
1	175.27 ± 0.074	97.2 ± 0.007	175.4 ± 0.036	97 ± 0.0065
2	176.4 ± 0.006	97.17 ± 0.085	176.51 ± 0.08	96.9 ± 0.049
3	177 ± 0.027	96.82 ± 0.064	177.2 ± 0.071	96.8 ± 0.03

Values given as mean ± standard deviation, $n = 3$

EE entrapment efficiency

In vivo pharmacokinetic and brain distribution studies

The pharmacokinetic parameters following IN and IV administration of LH drug solution and LHMM in Wistar rats are represented in Table 2 and the plasma concentration vs. time graphs in Fig. 7. The IN administration of LHMM showed highest brain concentrations of 9.5 ± 0.21 μg/ml at similar T_{max} of 1 h. This increased bioavailability of LH in the brain post IN administration using LHMM could be ascribed to nanosize and the surfactant properties the mixed micelles [35]. Also, a significant 4.5-fold increase ($p < 0.001$) in C_{max} for LHMM than pure drug in plasma was observed after IV administration. Thus, enhanced LH solubility in hydrophilic polymeric network of mixed micelles improved its bioavailability in plasma as well. However, the presence of blood-brain barrier (BBB) in intravenous route allowed less amount of drug to reach brain, the site of action for LH [34, 35]. Tissue distribution studies showed that the C_{max} attained in brain tissue following nasal intake was significantly superior to the C_{max} achieved via IV route indicating the effectiveness of LHMM in brain targeting via nasal administration [36]. Nanosized mixed micellar carriers are effective in transporting active moieties to the brain via intracellular and extracellular transports as well as passing through the olfactory pathway [37, 38].

Literature reports explained that the drug given by nasal pathway can reach the brain chiefly by two passageways: by crossing BBB after achieving therapeutic levels in blood circulation or by direct passage through nasal cavity from trigeminal nerve and olfactory region evading BBB [39, 40]. Two parameters, i.e. %DTE and %DTP, prove direct brain targeting of LH through the second passageway as mentioned above. %DTE signify time average drug partitioning between blood and brain while %DTP imply drug proportion transported to the brain via olfactory and trigeminal neural pathway, directly [41]. As shown in Table 3, there was 3.6-fold ($p < 0.01$) and 12.3-fold ($p < 0.01$) increase in %DTE and %DTP, respectively. It is well reported that GL44, derived from the mixtures of mono, di and triglycerides with PEG esters of fatty acids can inhibit Pgp efflux transporters present at the cerebrovascular endothelial cell membranes for enhancing the drug bioavailability in the brain tissue [35]. This highlighted the advantage of formulating LH as LHMM for improved bioavaibility in brain using intranasal route.

Stability studies

Stability studies of optimized LHMM at room temperature and accelerated stability conditions exhibited no significant change in micellar size as well as encapsulation efficiency post 3 months (Table 4). At accelerated stability conditions, there is possibility of collision of particles due to increased kinetic energy. However, hydrophilic PF127 like pluronic copolymers provide steric hindrance for kinetic stability as well as prevent micellar aggregation [36].

Conclusion

Stable lurasidone mixed micelles having 175 nm particle size and 97.8% entrapment efficiency were prepared by solvent evaporation method successfully. Optimum amount of Gelucire 44/14 and Pluronic F127 resulted in spherical, nanosized mixed lurasidone micelles by means of factorial design optimization. Mixed micelles improved the brain distribution as well as kinetics of lurasidone via intranasal route. In vitro diffusion and ex vivo permeation studies across nasal membrane showed sustained release of lurasidone hydrochloride from micelles with better permeability and brain bioavailability. Intact sheep nasal mucosa post micellar treatment exhibited the safety of formulated mixed micelles. In vivo brain distribution studies in rats emphasized the superiority of lurasidone entrapped mixed micelles for brain targeting by intranasal route than intravenous route. Nanosize of mixed micelles allowed drug to reach brain tissue via olfactory and trigeminal systems, bypassing the blood-brain barrier (BBB). In brief, intranasal delivery of lurasidone mixed micelles

possess the potential to address the challenges of extensive first pass metabolism, need of food for absorption from gastrointestinal tract and less oral bioavailability of lurasidone. Hence, micellar-based polymeric systems at nanoscale are apt carriers for effective nose-to-brain delivery of lurasidone hydrochloride. These systems would definitely facilitate the clinical translation of many neurotherapeutic actives used in the treatment of psychotic disorders.

Compliance with ethical standards The authors declare that the animal experiments described in this manuscript were performed in compliance with the existing ethical and institutional guidelines for the care and use of laboratory animals in India.

Conflict of interest The authors declare that they have no conflicts of interest.

References

1. Miao Y, Sun J, Chen G, Lili R, Ouyang P. Enhanced oral bioavailability of lurasidone by self-nanoemulsifying drug delivery system in fasted state. Drug Dev Ind Pharm. 2016;42(8):1234–40. https://doi.org/10.3109/03639045.2015.1118496.
2. Jaeschke RR, Sowa-Kućma M, Pańczyszyn-Trzewik P, Misztak P, Styczeń K, Datka W. Lurasidone: the 2016 update on the pharmacology, efficacy and safety profile. Pharmacol Rep. 2016;68(4):748–55. https://doi.org/10.1016/j.pharep.2016.04.002.
3. Shah S, Parmar B, Soniwala M. Chavda1 J. Design, optimization, and evaluation of lurasidone hydrochloride nanocrystals. AAPS PharmSciTech. 2016;17(5):1150–8. https://doi.org/10.1208/s12249-015-0449-z.
4. Fornaro M, De Berardis D, Perna G, Solmi M, Veronese N, Orsolini L, et al. Lurasidone in the treatment of bipolar depression: systematic review of systematic reviews. Biomed Res Int. 2017;2017:3084859. https://doi.org/10.1155/2017/3084859.
5. Lee K, Chae Y, Koo T. Pharmacokinetics of lurasidone, a novel atypical anti-psychotic drug, in rats. Xenobiotica. 2011;41(12):1100–7. https://doi.org/10.3109/00498254.2011.603388.
6. Qian S, Heng W, Wei Y, Zhang J, Gao Y. Coamorphous lurasidone hydrochloride–saccharin with charge-assisted hydrogen bonding interaction shows improved physical stability and enhanced dissolution with pH-independent solubility behavior. Cryst Growth Des. 2015;15(6):2920–8. https://doi.org/10.1021/acs.cgd.5b00349.
7. Madan JR, Pawar KT, Dua K. Solubility enhancement studies on lurasidone hydrochloride using mixed hydrotropy. Int J Pharm Investig. 2015;5(2):114–20. https://doi.org/10.4103/2230-973X.153390.
8. Jangipuria FO, Londhe VA. Solubility enhancement of lurasidone hydrochloride by preparing SMEDDS. Int J Pharm Pharm Sci. 2015;7:283–8.
9. Dondapati D, Srimathkandala MH, Sanka K, Bakshi V. Improved solubility and dissolution release profile of lurasidone by solid self-nanoemulsifying drug delivery system. Anal Chem Lett. 2016;6(2):86–97. https://doi.org/10.1080/22297928.2016.1164075.
10. Yu P, Lu S, Zhang S, Zhang W, Li Y, Liu J. Enhanced oral bioavailability and diminished food effect of lurasidone hydrochloride nanosuspensions prepared by facile nanoprecipitation based on dilution. Powder Technol. 2017;312:11–20. https://doi.org/10.1016/j.powtec.2017.02.038.
11. Jazuli I, Annu, Nabi B, Moolakkadath T, Alam T, Baboota S, et al. Optimization of nanostructured lipid carriers of lurasidone hydrochloride using box-behnken design for brain targeting: in vitro and in vivo studies. J Pharm Sci. 2019:1–9. https://doi.org/10.1016/j.xphs.2019.05.001.
12. Grassin-Delyle S, Buenestado A, Naline E, Faisy C, Blouquit-Laye S, Couderc LJ, et al. Intranasal drug delivery: an efficient and non-invasive route for systemic administration: focus on opioids. Pharmacol Ther. 2012;134(3):366–79. https://doi.org/10.1016/j.pharmthera.2012.03.003.
13. Rashed HM, Shamma RN, Basalious EB. Contribution of both olfactory and systemic pathways for brain targeting of nimodipine-loaded lipo-pluronics micelles: in vitro characterization and in vivo biodistribution study after intranasal and intravenous delivery. Drug Deliv. 2017;24(1):181–7. https://doi.org/10.1080/10717544.2016.1236848.
14. Cagel M, Tesan FC, Bernabeu E, Salgueiro MJ, Zubillaga MB, Moretton MA, et al. Polymeric mixed micelles as nanomedicines: achievements and perspectives. Eur J Pharm Biopharm. 2017;113:211–28. https://doi.org/10.1016/j.ejpb.2016.12.019.
15. Salama AH, Shamma RN. Tri/tetra-block co-polymeric nanocarriers as a potential ocular delivery system of lornoxicam: in-vitro characterization, and in-vivo estimation of corneal permeation. Int J Pharm. 2015;492:28–39. https://doi.org/10.1016/j.ijpharm.2015.07.010.
16. Jaiswal M, Kumar M, Pathak K. Zero order delivery of itraconazole via polymeric micelles incorporated in situ ocular gel for the management of fungal keratitis. Colloids Surf B: Biointerfaces. 2015;130:23–30. https://doi.org/10.1016/j.colsurfb.2015.03.059.
17. Kanade R, Boche M, Pokharkar V. Self-assembling raloxifene loaded mixed micelles: formulation optimization, in vitro cytotoxicity and in vivo pharmacokinetics. AAPS PharmSciTech. 2018;19(3):1105–15. https://doi.org/10.1208/s12249-017-0919-6.
18. Attia A, Yang C, Tan J, Gao S, Williams D, Hedrick J, et al. The effect of kinetic stability on biodistribution and anti-tumor efficacy of drug-loaded biodegradable polymeric micelles. Biomaterials. 2013;34(12):3132–40. https://doi.org/10.1016/j.biomaterials.2013.01.042.
19. Patil S, Choudhary B, Rathore A, Roy K, Mahadik K. Enhanced oral bioavailability and anticancer activity of novel curcumin loaded mixed micelles in human lung cancer cells. Phytomedicine. 2015;22(12):1103–11. https://doi.org/10.1016/j.phymed.2015.08.006.
20. Alsarra IA, Hamed Y, Mahrous GM, El Maghraby GM, Al-Robayan AA, Alanazi FK. Mucoadhesive polymeric hydrogels for nasal delivery of acyclovir. Drug Dev Ind Pharm. 2009;35(3):352–62. https://doi.org/10.1080/03639040802360510.
21. Saha A, Giri N, Agarwal S. Silver nanoparticle based hydrogels of tulsi extracts for topical drug delivery. International Journal of Ayurveda and Pharma Research. 2017;5(1):17–23.
22. Gambhire M, Jadhav K. Formulation, development and optimization of polymeric micelles of Telmisartan for enhancement of solubility using 3^2 factorial design. Int J ChemTech Res. 2017;10(10):298–310.
23. Seju U, Kumar A, Sawant K. Development and evaluation of olanzapine-loaded PLGA nanoparticles for nose-to-brain delivery: in vitro and in vivo studies. Acta Biomater. 2011;7(12):419–76.
24. Gaucher G, Dufresne M, Sant V, Kang N, Maysinger D, Leroux J. Block copolymer micelles: preparation, characterization and application in drug delivery. J Control Release. 2005;109:169–88.
25. Kallakunta V, Eedara B, Jukanti R, Ajmeera R, Bandari S. A Gelucire 44/14 and labrasol based solid self-emulsifying drug delivery system: formulation and evaluation. J Pharm Investig. 2013;43:185–96.
26. Jannin E, Pochard E, Chambin O. Influence of poloxamers on the dissolution performance and stability of controlled-release formulations containing Precirol1 ATO 5. Int J Pharm. 2006;309:6–15. https://doi.org/10.1016/j.ijpharm.2005.10.042.

27. Dhapte V, Pokharkar V. Polyelectrolyte stabilized antimalarial nanosuspension using factorial design approach. J Biomed Nanotechnol. 2011;7:139–41. https://doi.org/10.1166/jbn.2011.1239.
28. Jain R, Nabar S, Dandekar P, Hassan P, Aswal V, Talmon Y, et al. Formulation and evaluation of novel micellar nanocarrier for nasal delivery of sumatriptan. Nanomedicine (London). 2010;5(4):575–87. https://doi.org/10.2217/nnm.10.28.
29. Kumar R, Sai Ratan S, Nethravathi P. Development and characterization of oral disintegrating tablet containing nanosuspension of lurasidone hydrochloride antipsychotic drug. Asian J Pharm. 2017;11:102–11. https://doi.org/10.22377/ajp.v11i02.1153.
30. Dhapte V, Kadam V, Pokharkar V. Pyrimethamine nanosuspension with improved bioavailability: in vivo pharmacokinetic studies. Drug Deliv Transl Res. 2013;3(5):416–20. https://doi.org/10.1007/s13346-012-0112-0.
31. Patravale VB, Date AA, Kulkarni RM. Nanosuspensions: a promising drug delivery strategy. J Pharm Pharmacol. 2004;56:827–40. https://doi.org/10.1211/0022357023691.
32. Alam S, Khan ZI, Mustafa G, Kumar M, Islam F, Bhatnagar A, et al. Development and evaluation of thymoquinone-encapsulated chitosan nanoparticles for nose-to-brain targeting: a pharmacoscintigraphic study. Int J Nanomedicine. 2012;7:5705–18.
33. Majithiya RJ, Ghosh PK, Umrethia ML, Murthy RS. Thermoreversible-mucoadhesive gel for nasal delivery of sumatriptan. AAPS PharmSciTech. 2006;7(3):E80–6. https://doi.org/10.1208/pt070367.
34. Pokharkar VB, Jolly MR, Kumbhar DD. Engineering of a hybrid polymer-lipid nanocarrier for the nasal delivery of tenofovir disoproxil fumarate: physicochemical, molecular, microstructural, and stability evaluation. Eur J Pharm Sci. 2015;71:99–111. https://doi.org/10.1016/j.ejps.2015.02.009.
35. Pokharkar V, Patil-Gadhe A, Palla P. Efavirenz loaded nanostructured lipid carrier engineered for brain targeting through intranasal route: in-vivo pharmacokinetic and toxicity study. Biomed Pharmacother. 2017;94:150–64. https://doi.org/10.1016/j.biopha.2017.07.067.
36. Abdelbary GA, Tadros MI. Brain targeting of olanzapine via intranasal delivery of core-shell difunctional block copolymer mixed nanomicellar carriers: in vitro characterization, ex vivo estimation of nasal toxicity and in vivo biodistribution studies. Int J Pharm. 2013;452(1–2):300–10. https://doi.org/10.1016/j.ijpharm.2013.04.084.
37. Illum L. Transport of drugs from the nasal cavity to central nervous system. Eur J Pharm Sci. 2000;11:1–18.
38. Jain R, Nabar S, Dandekar P, Patravale V. Micellar nanocarriers: potential nose-to-brain delivery of zolmitriptan as novel migraine therapy. Pharm Res. 2010;27(4):655–64. https://doi.org/10.1007/s11095-009-0041-x.
39. Lochhead JJ, Thorne RG. Intranasal delivery of biologics to the central nervous system. Adv Drug Deliv Rev. 2012;64(7):614–28. https://doi.org/10.1016/j.addr.2011.11.002.
40. Md S, Khan RA, Mustafa G, Chuttani K, Baboota S, Sahni JK, et al. Bromocriptine loaded chitosan nanoparticles intended for direct nose to brain delivery: pharmacodynamic, pharmacokinetic and scintigraphy study in mice model. Eur J Pharm Sci. 2013;48(3):393–405. https://doi.org/10.1016/j.ejps.2012.12.007.
41. Nour SA, Abdelmalak NS, Naguib MJ, Rashed HM, Ibrahim AB. Intranasal brain-targeted clonazepam polymeric micelles for immediate control of status epilepticus: in vitro optimization, ex vivo determination of cytotoxicity, in vivo biodistribution and pharmacodynamics studies. Drug Deliv. 2016;23(9):3681–95. https://doi.org/10.1080/10717544.2016.1223216.